Hindawi
Complexity
Volume 2018, Article ID 8682725, 11 pages
https://doi.org/10.1155/2018/8682725

Research Article

Analysis of Converter Combustion Flame Spectrum Big Data Sets Based on HHT

Jincai Chang[1], **Jiecheng Wang**[1], **Zhuo Wang**[1], **Shuaijie Shan**[2] and **Chunfeng Liu**[1]

[1]*College of Sciences, North China University of Science and Technology, Tangshan 063210, China*
[2]*College of Electrical Engineering, North China University of Science and Technology, Tangshan 063210, China*

Correspondence should be addressed to Zhuo Wang; wz0910@126.com

Received 5 April 2018; Revised 10 May 2018; Accepted 16 May 2018; Published 5 June 2018

Academic Editor: Zhihan Lv

The characteristics of the converter combustion flame are one of the key factors in the process control and end-point control of steelmaking. In a big data era, it is significant to carry out high-speed and effective processing on frame spectrum data. By installing data acquisition devices at the converter mouth and separating the spectrum according to the wave length, high-dimensional converter flame spectrum big data sets are achieved. The data of each converter is preprocessed after information fusion. By applying the SM software, the correspondence with the carbon content is obtained. Selecting the relative data of the two peak ratios and the single-peak absolute data as a one-dimensional signal, due to the obvious nonlinear and nonstationary characteristics, using HHT to do empirical mode decomposition and Hilbert spectrum analysis, the variation characteristics after 70% of the converter steelmaking process are obtained. From data acquisition, data preprocessing to data analysis and results, it provides a new perspective and method for the study of similar problems.

1. Introduction

Converter steelmaking is currently the main steel production method. Under the condition of China's steel scrap shortage, converter steelmaking will be dominant for a long time [1]. Oxygen converter steelmaking reduces the carbon content in molten iron and raises the temperature. By blowing high-pressure and high-purity oxygen from the oxygen lance at the top of the converter, the molten steel can meet the target requirements of composition and temperature. Therefore, the establishment of an end-point prediction model with strong adaptability and high hit rate is of great significance for ensuring the quality of molten steel, reducing costs, and improving the production efficiency of steelmaking.

The traditional end-point carbon content and temperature forecast is based on the mechanism model of the mass balance and heat balance during the oxygen-blown carbon process [2]. In recent years, some new end-point prediction methods have emerged, such as smelting noise analysis, pattern recognition, and texture analysis [3]. Because the light intensity spectrum of the converter will show certain rules along with the process of blowing, as the accurate theory of light intensity spectrum detection matures [4], there have been many attempts to use optical methods to judge the end point of converter steelmaking. Professor Yanru Chen of Nanjing University of Science and Technology found that the light intensity and image characteristic information have remarkable changes in the steelmaking blowing process and established the end-point time mathematical model using regression analysis method [5]. Bethlehem Inc. of the United States has successfully developed an optical probe that measures the carbon content of the molten steel by measuring the amount of oxygen blown into the converter and the difference in light intensity of discharge furnace gas. At present, it is only applicable for the control of the end-point carbon content of molten steel with a carbon content of less than 0.05% in large-scale converters with oxygen supply stability of over 200 t, and there are cumbersome cooling devices in the plant [6]. Small- and medium-sized converter production accounts for about 75% of the total in

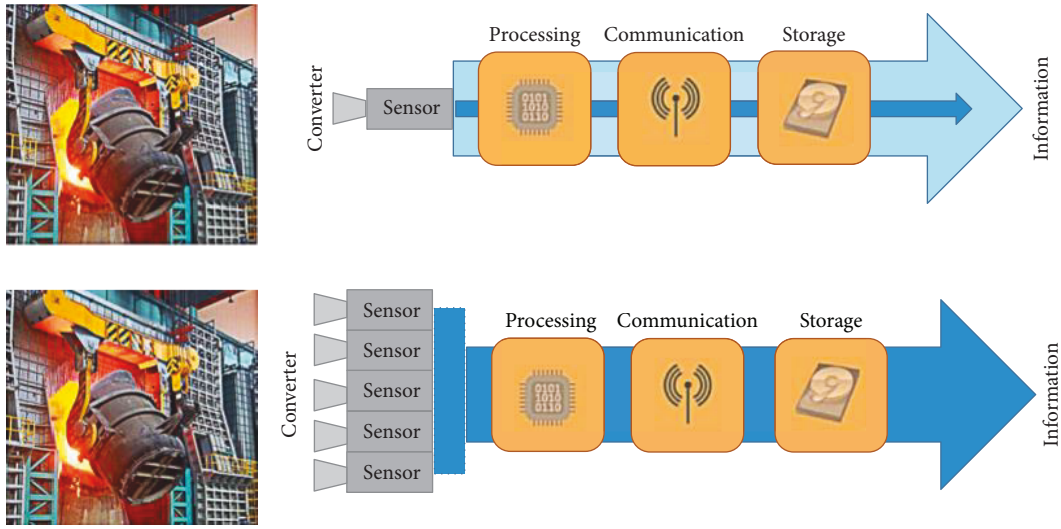

Figure 1: The performance bottleneck of signal processing.

China at present. The most commonly used of these plants is the empirical steelmaking method [7], which is a static control based on material balance and heat balance. In the production, it is often necessary to melt down, which makes it difficult to ensure a high hit rate, resulting in waste of resources and inefficiency.

In the past 30 years, the theory, methods, and techniques of signal processing have been developing, expanding, and deepening. With the progress of signal processing theory, hardware technology, and system technology, signal acquisition has now entered a diversified big data era [8]. The signal has evolved from one-dimensional signals to high-dimensional signals. The multispectral image to be processed is a high-dimensional signal with a large amount of data. The rapid development of the signal in terms of bandwidth, dimension, resolution, and acquisition network makes the growth rate of signal acquisition data higher than the growth rate of data storage and signal processing speed [9]. In the past, a major problem for converter flame signal processing researchers to study the end-point prediction was the "signal collection bottleneck": the amount of signal collected by the sensor system was too small, making subsequent information extraction and interpretation difficult and complex. For this reason, signal processing workers have been working on two aspects. On the one hand, less data is used to do as much as possible, and on the other hand, more abundant signal data is managed to be collected [10]. In the context of big data, the bottleneck of signal processing has shifted from "too little signal acquisition" to "how to handle massive amounts of signal data at high speed" (Figure 1). In the background of a big data era, traditional methods of flame spectral signal processing cannot quickly and efficiently excavate the useful information contained in the flame spectrum big data sets. A large amount of valuable data is wasted. It is necessary to study signal processing methods based on big data methods to analyse the frame spectrum.

In view of the above-mentioned status quo and existing problems at home and abroad, it is urgent to develop an accurate, low-cost, real-time, high-efficiency, and easy-to-operate end-point control method suitable for most converters in the context of big data. The flame spectral signal is a typical nonlinear, nonstationary time-varying big data signal that contains a rich frequency component [11]. Using traditional spectrum analysis methods, it is difficult to analyse it rationally, and it is impossible to accurately reveal the details of time-frequency changes. In order to successfully complete the feature extraction, it is necessary to introduce a more effective time series analysis method.

In order to deal with nonlinear, nonstationary big data signals better, many scholars have proposed many new signal processing methods in recent years, among which the more famous is the empirical mode decomposition (EMD). This method was proposed by Huang et al. in 1998 and is very suitable for the analysis and processing of time series with nonlinear and nonstationary features [12]. It is considered as a major breakthrough in signal processing in recent years. At present, the method has been widely used in the fields of economics, geophysics, oceanography, biomedicine, power system fault signal analysis, and mechanical fault diagnosis and has achieved good results [13].

Compared with the current end-point prediction method for converter steelmaking, the use of the HHT method has certain advantages. The static state model calculates the content of carbon according to the chemistry reaction in the pudding and the initialized content of carbon in the melt iron. However, the static model cannot be used in the dynamic condition; measuring the carbon emitted spectrum of the exhaust gas in the furnace to calculate the content of carbon costs a lot; Bethlehem's proposal has low accuracy. The HHT method has advantages such as low cost and high accuracy. Moreover, it can also be applied to the dynamic condition.

The spectral information of the steelmaking process is short-term, transient, nonperiodic, nonlinear, and nonstationary. Combining the outstanding performance of the

EMD method and HHT transform in nonlinear nonstationary big data signal processing, we propose a HHT-based spectral analysis method in the context of big data. We collect the frame spectrum image information from one steel industry and analyse the signal characteristics of the spectrum of the steelmaking process. Through the EMD and HHT transformation [14], the characteristic points of the spectrum of the steelmaking process are searched, and the ultimate goal of the steelmaking end prediction is achieved. It provides a new path and method for the transformation and value creation of Chinese steel companies in the Industry 4.0 era.

2. Implementation Process of HHT

Traditional signal analysis and processing are based on Fourier analysis. They are applicable to linearity, Gaussianity, and stationarity. And they establish an idealized model. HHT overcomes the shortcomings of traditional signal analysis methods and is suitable for handling nonlinear and nonstationary signals and is adaptive. According to the characteristics of the signal, the signal is decomposed into several IMF components, which has good adaptability and time-frequency aggregation.

2.1. Definition of Intrinsic Mode Function (IMF). The intrinsic mode function (IMF) must satisfy the following two conditions:

(1) Over the entire data range, the difference number of extreme points and zero crossings is zero or one.

(2) At any point, the average of the envelope formed by all the maximum points and the envelope formed by all the minimum points is zero.

The IMF component has significant characteristics of slowly varying wave packets. Each IMF component is a stationary signal with nonlinear characteristics. Its slowly varying wave packet characteristics mean that the wave amplitudes of different characteristic scale fluctuations change with time. Therefore, it also has the characteristics of localization in the time domain.

2.2. The Algorithm of Empirical Mode Decomposition (EMD). Empirical mode decomposition (EMD) is proposed by N. E. Huang et al. The IMF component obtained by EMD satisfies the conditions required by the Hilbert transformation, so the original data needs to be decomposed by the EMD method. The EMD process is the process of decomposing the nonlinear unstable signal from high frequency to low frequency into multiple IMFs. It is also the process of signal stabilization, and the frequency resolution included in each IMF also changes with the original signal. It is a kind of adaptive multi-resolution signal processing method.

The basic principle of EMD can be described as follows:

(1) Determine the local minima and maxima of time series $X(t)$.

(2) The local minima and maxima of $X(t)$ are respectively fitted with cubic spline curves to form upper and lower envelopes, $X_{\max}(t)$ and $X_{\min}(t)$, and mean values $m(t)$ are calculated.

(3) Let $h(t) = X(t) - m(t)$ and compare with the IMF condition; if it meets the condition, $h(t)$ is the IMF-1 component of $X(t)$, record as $C_1(t)$, then get the residual function $r(t) = X(t) - C_1(t)$. Let $r(t)$ be a new $X(t)$ and repeat processes (1)–(3); if it does not meet the conditions, let $h(t)$ be a new $X(t)$ and repeat processes (1)–(3).

(4) Repeat procedures (1) through (3) until the residual function $r(t)$ is a monotonic function or constant.

The time series $X(t)$ is decomposed into several intrinsic mode functions and one residual quantity by EMD, which can be expressed as

$$X(t) = \sum_{i=1}^{n-1} C_i(t) + r_n(t). \tag{1}$$

The above method is the empirical mode decomposition (EMD).

2.3. Analysis of Hilbert Spectrum. A set of intrinsic mode functions are obtained by EMD, and then the Hilbert transformation is performed on each IMF to calculate the instantaneous frequency. Change i to j in formula (1):

$$X(t) = \sum_{j=1}^{n} C_j(t) + r_n. \tag{2}$$

A Hilbert transformation is applied to each intrinsic mode function $C_j(t)$ except the residual quantity r_n to obtain the data sequence $\bar{C}_j(t)$:

$$\bar{C}_j(t) = \frac{1}{\pi} P \int \frac{C_j(t)}{t-\tau}\, d\tau. \tag{3}$$

We can form a complex sequence by $C_j(t)$ and $\bar{C}_j(t)$

$$z_j(t) = c_j(t) + i\bar{c}_j(t) = a_j(t) e^{i\theta_j(t)}. \tag{4}$$

We get the instantaneous frequency as

$$\omega_j(t) = \frac{d\theta_j(t)}{dt}. \tag{5}$$

Therefore, the original data can be expressed as

$$X(t) = \mathrm{Re} \sum_{j=1}^{n} a_j(t) \exp\left(i \int \omega_j(t)\, dt \right), \tag{6}$$

where Re represents the real part; $r_n(t)$ is generally omitted because it is a monotonic function or constant.

According to (6), time t, frequency ω_j, and amplitude a_j can be plotted on a three-dimensional figure, which is

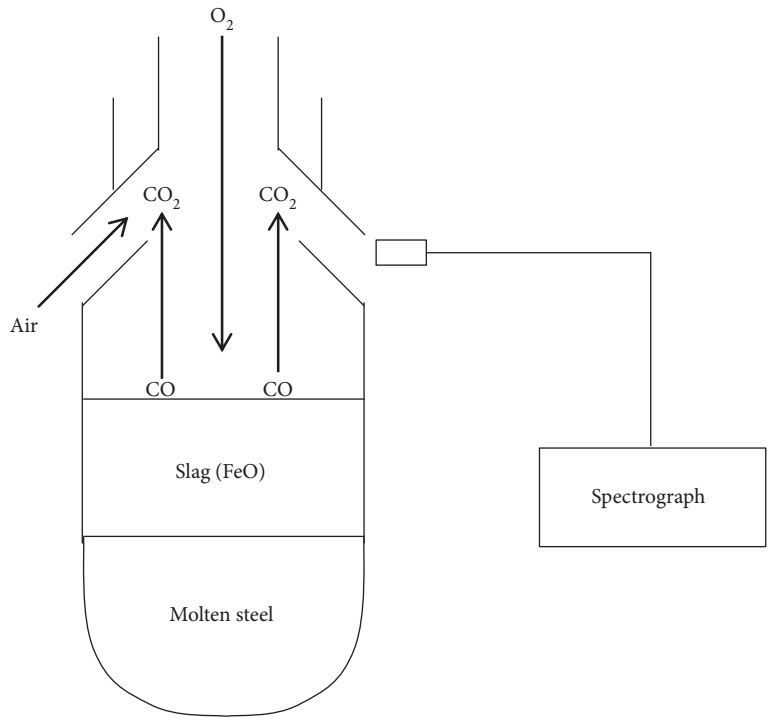

Figure 2: Schematic diagram of a basic oxygen furnace.

called the Hilbert amplitude spectrum and referred to as the Hilbert spectrum.

Mark the Hilbert spectrum as

$$H(t,f) = \mathrm{Re} \sum_{j=1}^{n} a_j(t) \exp\left(i \int \omega_j(t)\, dt\right). \tag{7}$$

Define the marginal spectrum as

$$h(f) = \int_0^T H(t,f)\, dt, \tag{8}$$

where T is the total length of the signal, $H(t,f)$ is the variation of the amplitude of the signal over the entire frequency band and the frequency, and $h(f)$ is the variation of the amplitude of the signal with the frequency over the entire frequency band.

3. Big Data Processing in Converter Steelmaking Process

3.1. Technological Process of Converter Steelmaking. The traditional converter steelmaking process is to mix molten iron after steelmaking through a mixer furnace, then pour it into a converter and insert a water-cooled oxygen lance into the converter to convert it to a certain oxygen pressure, gun position, and slagging system. When the operator estimates that the end of the blowing is reached, the oxygen gun is raised, the converter is inverted to a certain position, and the composition and temperature of the molten steel are sampled and measured. If the molten steel composition and temperature do not reach the target range, the water-cooled oxygen lance needs to be reinserted into the converter and slag-forming. The above steps are repeated until the molten steel reaches the target range. In the conventional converter process, the oxygen top blowing converter has always been dominant. The main function of the process shown in Figure 2 is oxidating carbon content in molten iron, so that the carbon content in the converter can meet the requirements. By increasing the molten steel temperature by a large amount of exothermic reaction, the molten steel temperature requirement for secondary refining is satisfied.

3.2. Big Data Analysis of Spectral Information in Converter Steelmaking. In empirical control or dynamic control mode, workers must obtain varying degrees of information from changes in the flame. This information includes the light intensity, spectral distribution, and flame image information of the flame. In order to find the end of converter steelmaking, we first analyse the spectral information in the steelmaking process. A variation diagram of wavelength-time-flame intensity of the whole process is as shown in Figure 3.

In the early period of converter steelmaking, the colour of the flame is dark red, the brightness is low, and a large amount of smoke is present. In the midstage of converter steelmaking, the flame gradually becomes whitish, the brightness is obviously increased, and irregular jitter occurs, accompanied by small-scale shot-spraying. At the later stage of converter steelmaking, the flame is pale white, the brightness is the highest, the flame is relatively stable, and there is explosion sparks appear. Through the analysis of the flame at the late stage of steelmaking, although there will be metallic excitation lines (Na line and double K line), and small peaks appear in the vicinity of 800 mm, the overall flame

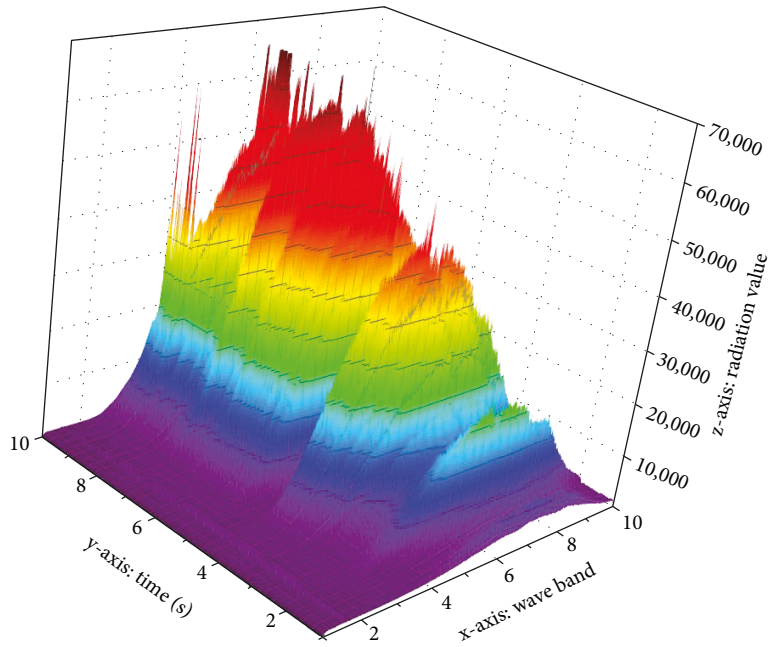

Figure 3: Variation diagram of wavelength-time-flame intensity of the whole process.

intensity is strong and does not need to feed the converter. Oxygen feeding is relatively stable, so the flame spectrum is relatively stable during this period. When predicting the end point of converter steelmaking, the spectrum of late steelmaking can be selected for analysis. This article selects the steelmaking process after 70% for analysis.

3.3. Converter Combustion Flame Spectrum Big Data Sets. In the process of metal smelting, the converter produces flame, then the optical information emitted by the flame is projected onto the photo detector through the theory of pinhole imaging. Next, according to the discrete frequency, the light intensity data of the flame is recorded at every 0.5 s by the photo detector.

First, the collected spectrum information is a data set, each column representing a specific frequency. Each row corresponds to the problem of the light intensity data set. The amount of data received by the photo detector is 2048 during every 0.5 seconds. It is a big data problem to use the values of these 2048 light intensities to predict the flame temperature and the content of the key elements in the raw materials in real time. The collected data sets are so voluminous and complex that traditional data processing application software is inadequate to deal with them. Therefore, in order to better reflect the characteristics of the collected data, in this article, we call the spectrum data set collected by the sensor in real time as "converter combustion flame spectrum big data sets." Converter combustion flame spectrum big data sets have 3V characteristics: volume, velocity, and value.

3.4. Information Fusion of Flame Spectrum. The data provided by the sensors installed in the converter ports may have problems such as repeated data redundancy, incomplete content, sparseness, and inaccuracy [15]. In order to extract useful, real-time, and accurate information from a large number of multicategory information to determine the end point of converter steelmaking, it is necessary to fuse the collected flame spectrum big data sets. The problems to be studied now have shifted from data lack to data enrichment. The flame spectral signal processing in the context of big data needs to firstly perceive compression to reduce the data volume of the signal and then multisensor information fusion to handle complex multisource information. Through smart sensor network technology, valuable signals are extracted. Finally, high-speed signal processing improves signal processing speed. The whole process is as shown in Figure 4.

Since the object to be processed is the raw data information obtained by the sensor, we adopt a centralized processing information fusion structure. The data captured by each sensor will be transmitted directly to the fusion centre where the data is aligned and interconnected. The loss of information in a centralized system structure is relatively small. The specific implementation process is shown in Figure 5.

3.5. Processing of Converter Frame Spectrum Big Data Sets. During the steelmaking process, the spectrometer collects the light information of the flame in the converter and records the luminous intensity *f_1–f_2048* of different light frequencies every 0.5 seconds. The raw data also includes the time t, the Kelvin temperature T, the instantaneous oxygen blowing rate V_Q, and the primary carbon content C. The data of the oxygen lance position greater than 2.5 and the data of instantaneous oxygen rate less than 1000 are removed.

3.5.1. Content of Carbon. By the formula

$$Q_n = \frac{V_{Qn-0.5} + V_{Qn}}{2},$$
$$Q = \sum Q_n. \tag{9}$$

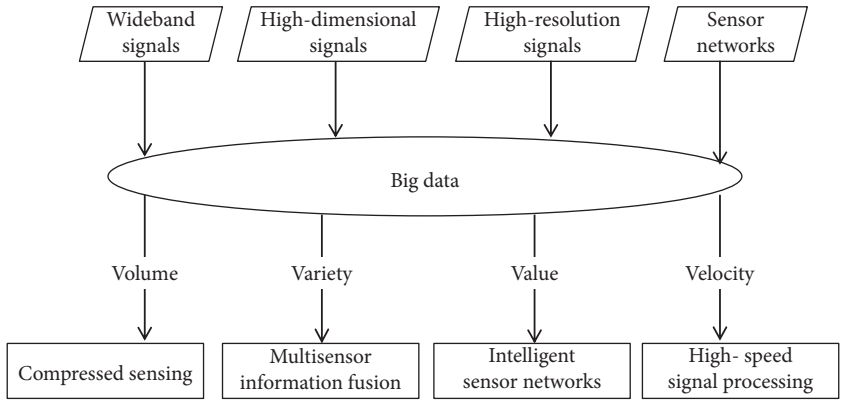

Figure 4: Signal processing in the context of big data.

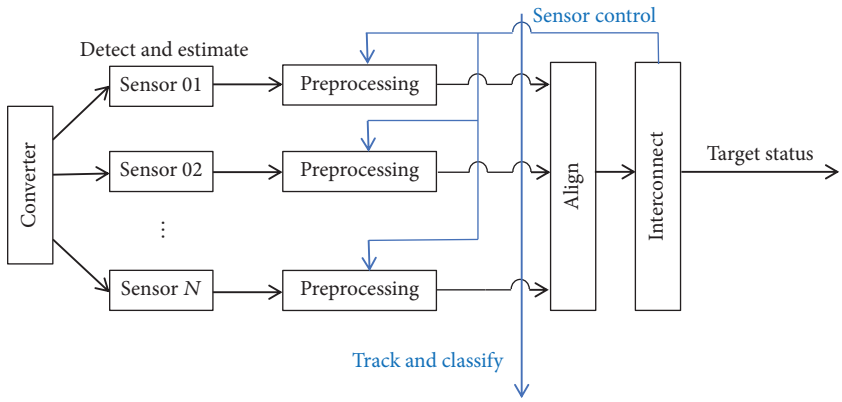

Figure 5: Centralized fusion system architecture.

We can obtain the cumulative oxygen blowing Q of the entire steelmaking process. Q_n indicates the average value of oxygen in the n second. $V_{Qn-0.5}$ and V_{Qn} represent the instantaneous oxygen blowing rate for the $n-0.5$ second and the n second, respectively.

The definition of cumulative oxygen consumption ratio

$$P = \frac{\sum_1^n Q_n}{Q}. \tag{10}$$

This article studies the cumulative oxygen consumption ratio in the 70% to 100% phase. According to the oxygen content and the amount of primary carbon in the collected data, the SM software provided by the steel company is used. This software can derive the value of the cumulative oxygen content with a step of 0.1 carbon content [16]. Through observation and judgment, the carbon content is linearly related to the cumulative oxygen blowing amount [17]. Using piecewise linear interpolation, the carbon content corresponding to each cumulative oxygen volume is determined.

3.5.2. Converter Flame Spectral Information. Analysis of the data of 20 converters revealed that when the accumulated oxygen consumption ratio is between 70% and 100%, there always exists two peaks and the wavelengths are similar and concentrated near a certain band, as shown in Figure 6.

In order to further explore the relationship between the carbon content and flame spectrum, peak light intensity (absolute intensity) and the ratio of the light intensities of the two relative peaks (relative intensity) are analysed as the signal. The signals obtained after two different processing methods are shown in Figures 7 and 8:

4. Analysis of Results

4.1. Intrinsic Mode Function (IMF). The EMD method is an adaptive signal processing method with a high signal-to-noise ratio [18]. Each intrinsic mode function (IMF) of the absolute intensity signal and the relative intensity signal is obtained by empirical mode decomposition. With the carbon content on the x-axis and the frequency of each IMF on the y-axis, all the IMF patterns for each converter are drawn. This article takes the converter 6C00582 as an example for analysis. To ensure accuracy, the original signal is decomposed into eight IMF components. The decomposition results of the absolute intensity signal and the relative intensity signal are shown in Figures 9 and 10.

There are eight IMF components in the figure, of which IMF-8 is a trend item. It can be seen from the figure that when absolute intensity signal is used as the signal for analysis, the first two-order components have obvious irregular fluctuations and the latter waveform gradually tends to

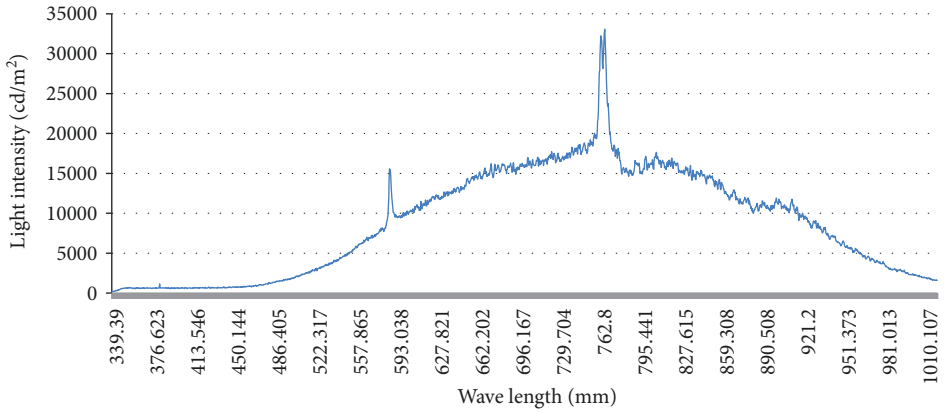

Figure 6: June 22, 2017, 18:37:00 converter 6C00582 light intensity-optical frequency diagram.

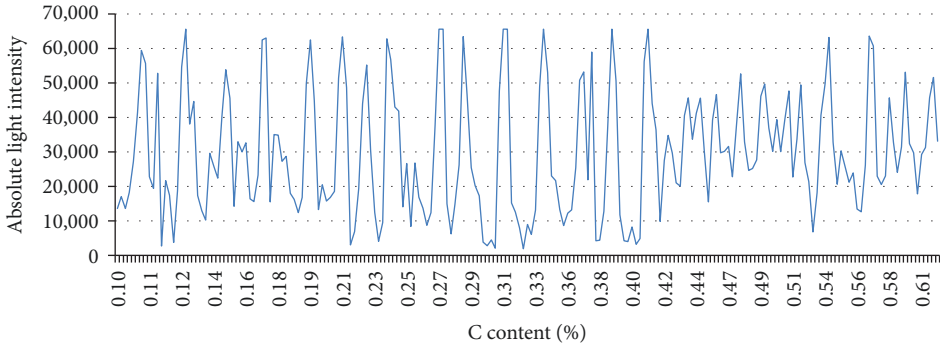

Figure 7: The signal diagram of the converter 6C00582 with absolute intensity as the original signal.

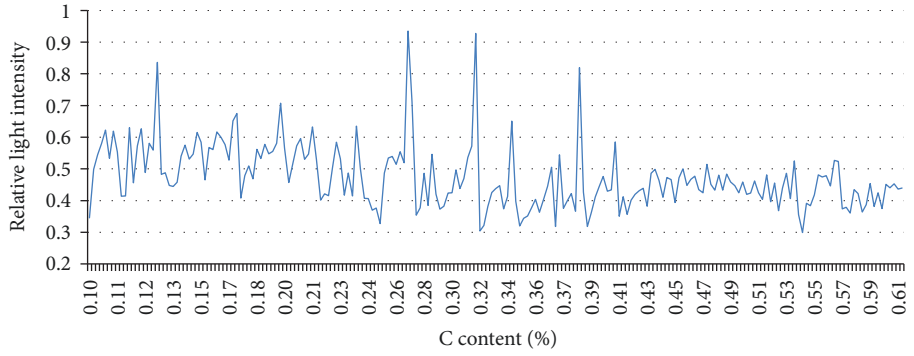

Figure 8: The signal diagram of the converter 6C00582 with relative intensity as the original signal.

ease; when relative intensity is used, the first three-order components have obvious irregular fluctuations. Afterwards, the waveform gradually became stable. It reflects that the characteristics of the high-frequency part of the absolute intensity signal are reflected in the first two-order components, the characteristics of the low-middle-frequency part are reflected in the later-order IMF components, and the characteristics of the high-frequency part of the relative intensity signal are in the first three-order components. The result shows that the relative intensity signal contains more high-frequency signals than the absolute intensity signal. The trend of IMF-8 reaction shows that with the decrease of carbon content, the frequency is increasing, which is consistent with the actual phenomenon, indicating that the use of empirical mode decomposition can accurately reflect the trend of changes in carbon content in steelmaking.

From the IMF component images derived from the original data and empirical mode decomposition (EMD), it can be concluded that the data composition and trend of the converter number 6C00582 is generally consistent with most of the other converters. It can be inferred that the converter's steelmaking raw materials are similar to the process [19]. By comparing the data of steelmaking raw materials, the conclusions are illustrated.

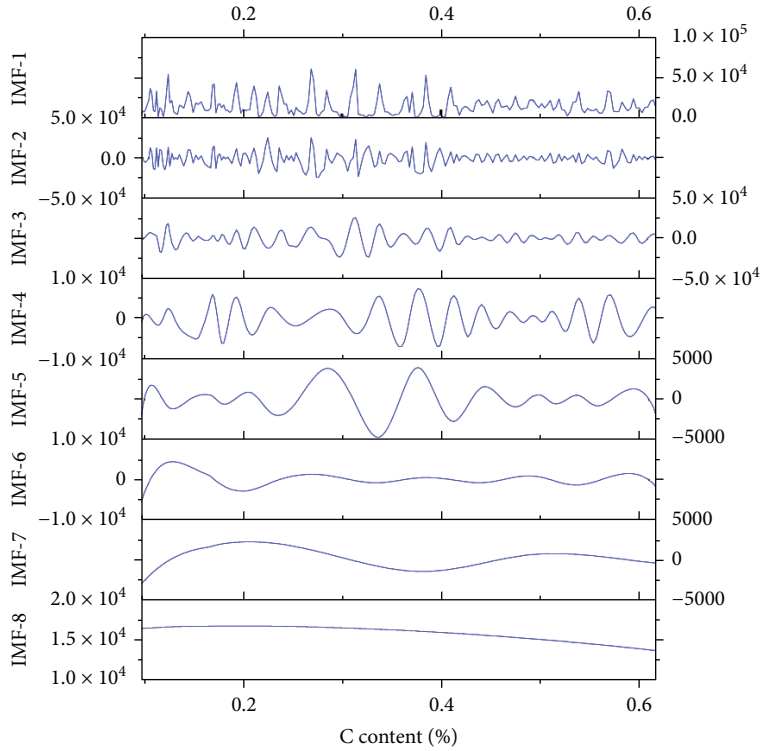

Figure 9: Carbon-IMF frequency diagram of converter 6C00582 signalled with absolute intensity.

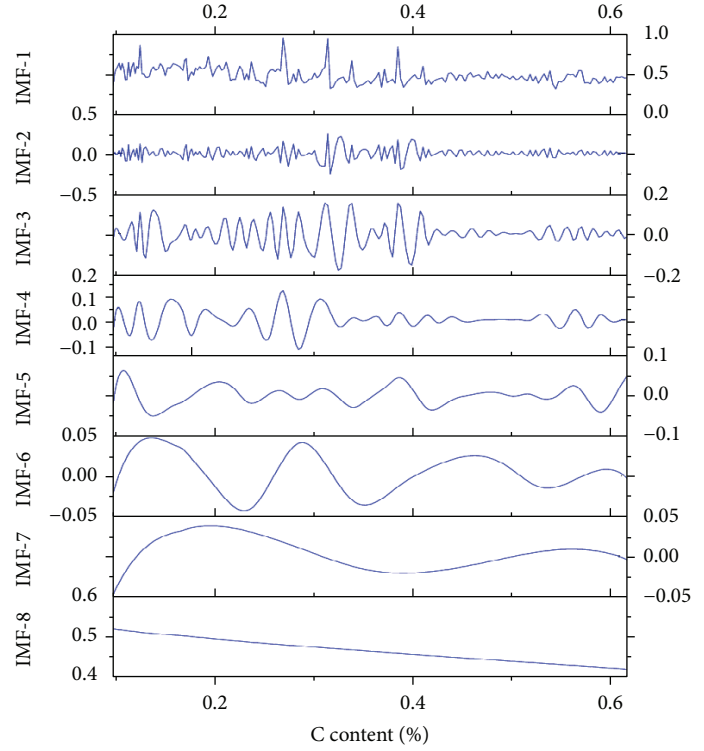

Figure 10: Carbon-IMF frequency diagram of converter 6C00582 signalled with relative intensity.

Mathematical data anomalies occur when dealing with some of the converter's raw data and IMF images. In the actual steelmaking process, the data anomalies may be due to differences in the quality and ratio of raw materials for steelmaking or accidental influencing factors in the steelmaking process.

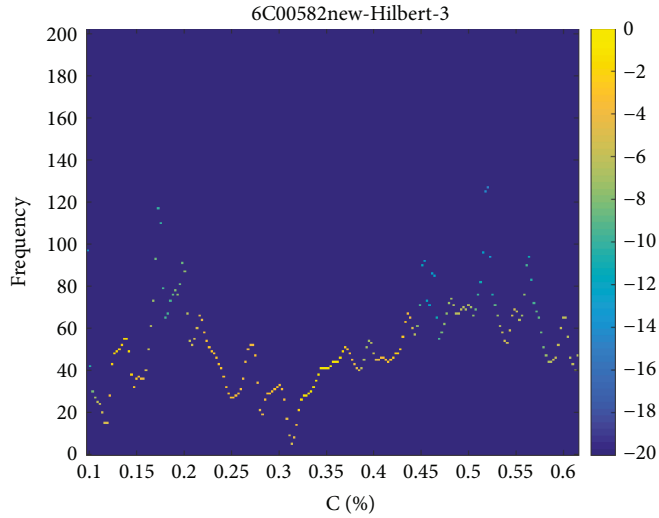

Figure 11: Hilbert spectrum diagram of IMF-3 signalled with absolute intensity.

4.2. Analysis of Hilbert Spectrum. The intrinsic mode functions of twenty converters' data are compared, and sixteen converters with valid data are selected. In the sixteen selected converters, eleven converters with stronger IMF laws are analysed. It is found that the relative brightness (the ratio of the peak value of the wavelength to the mean value) of the Na reaction will change significantly when the carbon content was around 0.3%.

The intrinsic mode function of converter number 6C00582 is selected for spectrum analysis. In the following, the absolute intensity signal and the relative intensity signal are respectively decomposed by EMD to obtain their intrinsic mode function. Hilbert transformation is performed on each intrinsic mode function to obtain the Hilbert spectrum and marginal spectrum, and the results of adopting two different signal selection methods are compared and analysed.

4.2.1. Analysis of Absolute Intensity Signal Hilbert Spectrum. The Hilbert spectrum diagram of IMF-3 signalled with absolute intensity is as shown in Figure 11.

From the absolute intensity signal's IMF-3 Hilbert spectrum, it can be known that the yellow energy band is a low energy band, which is concentrated in the frequency range of 0~70 Hz. When the carbon content is in the range of 0.15~0.2% and 0.5~0.55%, two blue high-energy spectra will appear, and the frequency signal is between 120 and 140 Hz. The energy is high. There exists an obvious low-frequency, low-energy moment when carbon content is in the range of 0.3%~0.35%. A marginal spectrum of IMF-3 signalled with absolute intensity is shown in Figure 12.

From the marginal spectrum, we can see that there are high peaks and high energy values in the frequency range of 100~200 Hz, which is consistent with the results of the above analysis of the Hilbert spectrum.

4.2.2. Analysis of Relative Intensity Signal Hilbert Spectrum. The Hilbert spectrum of IMF-3, which uses the ratio of the light intensities of the two relative peaks of the converter as the original signal, is shown in Figure 13.

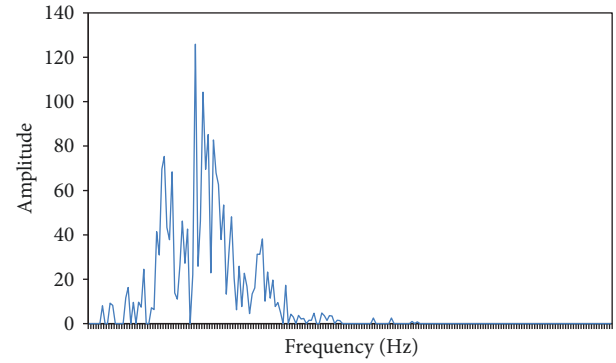

Figure 12: Marginal spectra of IMF-3 signalled with absolute intensity.

According to the Hilbert spectrum of IMF-3 signalled with relative intensity, the yellow energy is concentrated in the frequency range of 40~100 Hz, and the frequency signal between 40 and 100 Hz exists in the whole process; when the carbon content is in the range of 0.15~0.2% and 0.4–0.45%, two blue high-energy spectra will appear, the frequency signal is between 120 and 140 Hz, and the energy is relatively high. The IMF-3 marginal spectrum of the relative intensity signal is shown in Figure 14.

From the marginal spectrum, we can see that there are high peaks and high energy values in the frequency range of 100~200 Hz, which is consistent with the results of the above analysis of the Hilbert spectrum.

4.2.3. Comparison and Conclusion. Compared with the absolute intensity signal, the frequency signals of the two high-energy spectra of the relative intensity signal have shorter intervals and are closer to the time when the carbon content is 0.3%. With the absolute intensity signal, when the carbon content is close to 0.3%, low-frequency and low-energy phenomena occur. This provides an important basis for the predicting the end points of converter steelmaking.

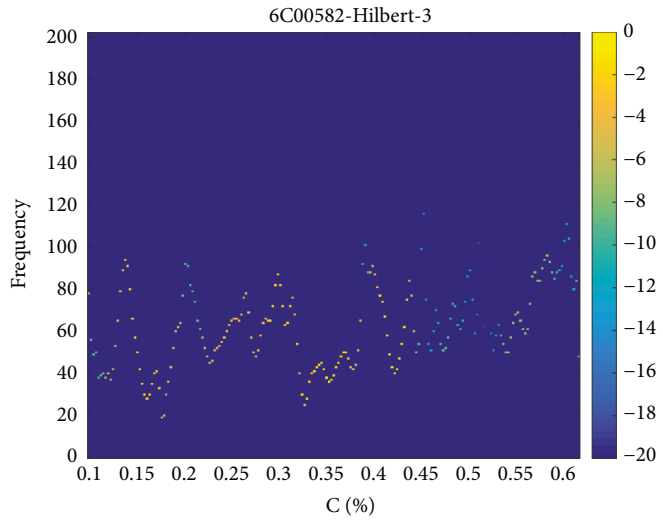

Figure 13: Hilbert spectrum diagram of IMF-3 signalled with relative intensity.

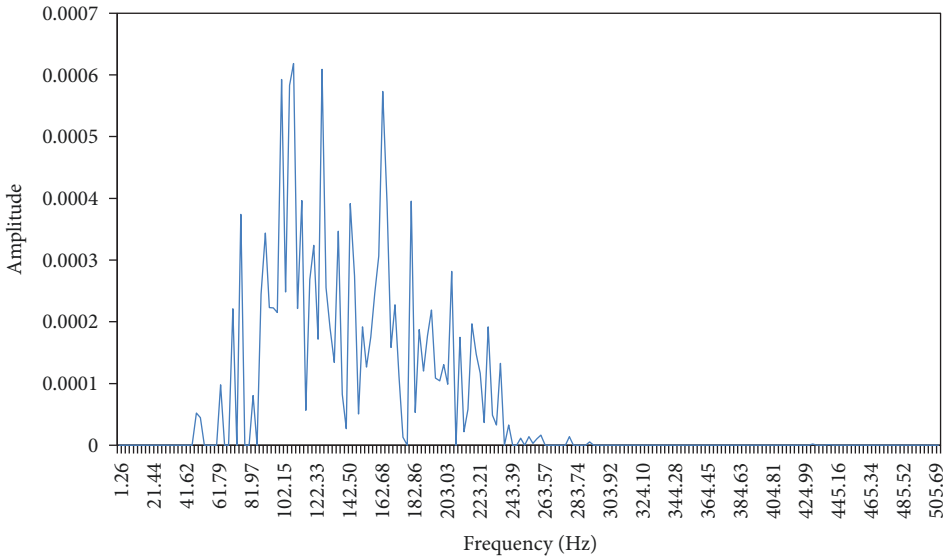

Figure 14: Marginal spectra of IMF-3 signalled with relative intensity.

The converter flame spectral information collected by the sensing device is transmitted to the computing device, and the computing device extracts in real time the ratio of the light intensity of the flame peak and the ratio of the light intensities of the two local peaks as the original signal and performs empirical mode decomposition and Hilbert transformation. First, observe IMF-3 Hilbert spectrum of the relative intensity signal. When a 120~140 Hz frequency signal appears, the carbon content has dropped to 0.4%, which is about to reach the end of the converter steelmaking; when the low-energy, low-frequency moment of the IMF-3 Hilbert spectrum of the absolute intensity signal appears, it means that the carbon content is about to drop to 0.3%, which has reached the end of converter steelmaking. At this point, it is necessary to stop the oxygen blowing process.

5. The Real-Time Prediction Test of the Model

In order to verify the validity of the HHT method for predicting the end point of the converter, the data of twenty converters are collected and simulated at the same time. The results are shown in Figure 15. The forecast result is ideal.

6. Conclusions

Faced with the pressures of international competition and domestic environmental governance, building intelligent factories is the only way for steel companies to transform, upgrade, and survive. Raising the final hit rate of steelmaking control and then achieving automatic steelmaking is an important link and goal for the construction of an intelligent steel company. This research is carried out in a steel

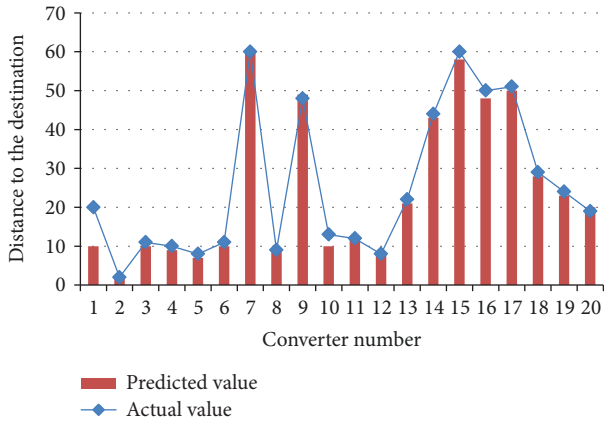

Figure 15: Distribution graph of the predicted value and the actual value.

company, and the flame spectrum big data sets are acquired by installing a data acquisition device at the mouth of the converter. After data preprocessing such as information fusion, the relative data of the ratio of the two peaks and the single peak absolute data are used as signals for the 70% flame after the steelmaking process of the company. Adaptive analysis is performed with HHT to achieve the spectrum change characteristics. The pretreatment, analysis methods, and results for such data have not been reported in other documents. It is an easy-to-execute, referential treatment method and has important reference value.

Data Availability

The data that support the findings of this study are available from the corresponding author upon reasonable request.

Conflicts of Interest

The authors declare that there is no conflict of interest regarding the publication of this paper.

Acknowledgments

This work was supported by the National Science Foundation of China (51674121, 61702184), the Returned Overseas Scholar Funding of Hebei Province (C2015005014), and the Hebei Key Laboratory of Data Science and Applications.

References

[1] Z. Qi, C. Gao, H. Na, and Z. Ye, "Using forest area for carbon footprint analysis of typical steel enterprises in China," *Resources, Conservation and Recycling*, vol. 132, pp. 352–360, 2018.

[2] H. Jalkanen and L. Holappa, "Converter steelmaking," *Treatise on Process Metallurgy*, vol. 3, pp. 223–270, 2014.

[3] H. Liu, B. Wang, and X. Xiong, "Basic oxygen furnace steelmaking end-point prediction based on computer vision and general regression neural network," *Optik - International Journal for Light and Electron Optics*, vol. 125, no. 18, pp. 5241–5248, 2014.

[4] A. Kumar and P. NandhaKumar, "OFDM system with cyclostationary feature detection spectrum sensing," *ICT Express*, 2018.

[5] Y. Shao, M. Zhou, Y. Chen, Q. Zhao, and S. Zhao, "BOF endpoint prediction based on the flame radiation by hybrid SVC and SVR modeling," *Optik - International Journal for Light and Electron Optics*, vol. 125, no. 11, pp. 2491–2496, 2014.

[6] A. Sharan, "Light sensors for BOF carbon control in low carbon heats," in *Steelmaking Conference Proceedings*, vol. 81, pp. 337–346, Toronto, Canada, 1998, Iron and Steel Society of AIME.

[7] J. Diao, et al.W. Zhou, Z. Ke et al., "System assessment of recycling of steel slag in converter steelmaking," *Journal of Cleaner Production*, vol. 125, pp. 159–167, 2016.

[8] R. G. Baraniuk, "More is less: signal processing and the data deluge," *Science*, vol. 331, no. 6018, pp. 717–719, 2011.

[9] J. Esteban, A. Starr, R. Willetts, P. Hannah, and P. Bryanston-Cross, "A review of data fusion models and architectures: towards engineering guidelines," *Neural Computing and Applications*, vol. 14, no. 4, pp. 273–281, 2005.

[10] B. Khaleghi, A. Khamis, F. O. Karray, and S. N. Razavi, "Multisensor data fusion: a review of the state-of-the-art," *Information Fusion*, vol. 14, no. 1, pp. 28–44, 2013.

[11] Y. Shao, Q. Zhao, Y. Chen, Q. Zhang, and K. Wang, "Applying flame spectral analysis and multi-class classification algorithm on the BOS endpoint carbon content prediction," *Optik - International Journal for Light and Electron Optics*, vol. 126, no. 23, pp. 4539–4543, 2015.

[12] N. E. Huang, Z. Shen, S. R. Long et al., "The empirical mode decomposition and the Hilbert spectrum for nonlinear and non-stationary time series analysis," *Proceedings of the Royal Society A: Mathematical, Physical and Engineering Sciences*, vol. 454, no. 1971, pp. 903–995, 1998.

[13] Z. M. Shi, L. Liu, M. Peng, C. C. Liu, F. J. Tao, and C. S. Liu, "Non-destructive testing of full-length bonded rock bolts based on HHT signal analysis," *Journal of Applied Geophysics*, vol. 151, pp. 47–65, 2018.

[14] N. E. Huang, M. L. C. Wu, S. R. Long et al., "A confidence limit for the empirical mode decomposition and Hilbert spectral analysis," *Proceedings of the Royal Society A: Mathematical, Physical and Engineering Sciences*, vol. 459, no. 2037, pp. 2317–2345, 2003.

[15] D. J. Brady, M. E. Gehm, R. A. Stack et al., "Multiscale gigapixel photography," *Nature*, vol. 486, no. 7403, pp. 386–389, 2012.

[16] A. Yang, Y. Han, Y. Pan, H. Xing, and J. Li, "Optimum surface roughness prediction for titanium alloy by adopting response surface methodology," *Results in Physics*, vol. 7, pp. 1046–1050, 2017.

[17] K. Cui and T. Zhao, "Unsaturated dynamic constitutive model under cyclic loading," *Cluster Computing*, vol. 20, no. 4, pp. 2869–2879, 2017.

[18] Y. G. Sun, H. Y. Qiang, J. Q. Xu, and D. S. Dong, "The nonlinear dynamics and anti-sway tracking control for offshore container crane on a mobile harbor," *Journal of Marine Science and Technology*, vol. 25, no. 6, pp. 656–665, 2017.

[19] A.-M. Yang, Y. Han, S.-S. Li, H.-W. Xing, Y.-H. Pan, and W.-X. Liu, "Synthesis and comparison of photocatalytic properties for Bi_2WO_6 nanofibers and hierarchical microspheres," *Journal of Alloys and Compounds*, vol. 695, pp. 915–921, 2017.